# Periodicity of the growth-band formation in vertebrae of juvenile scalloped hammerhead shark Sphyrna lewini from the Mexican Pacific Ocean

C. Coiraton, J. Tovar-Ávila, K. C. Garcés-García, J. A. Rodríguez-Madrigal, R. Gallegos-Camacho, D. A. Chávez-Arrenquín, and F. Amezcua

SEDAR77-RD38

Received: 9/8/2021

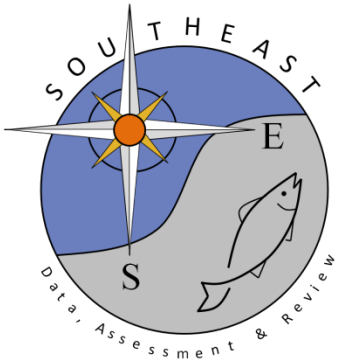

**REGULAR PAPER**

# Periodicity of the growth-band formation in vertebrae of juvenile scalloped hammerhead shark *Sphyrna lewini* from the Mexican Pacific Ocean

C. Coiraton[1] | J. Tovar-Ávila[2] | K. C. Garcés-García[3] | J. A. Rodríguez-Madrigal[4] | R. Gallegos-Camacho[5] | D. A. Chávez-Arrenquín[6] | F. Amezcua[7]

[1]Posgrado en Ciencias del Mar y Limnología, Universidad Nacional Autónoma de México; Av. Ciudad Universitaria 3000, Coyoacán, Mexico City, Mexico

[2]Centro Regional de Investigaciones Pesqueras Bahía Banderas. Calle Tortuga #1, La Cruz de Huanacaxtle, Bahía Banderas, Nayarit, Mexico

[3]University of Melbourne. Department of Zoology, Parkville, Victoria, Australia

[4]Pronatura Noroeste A.C. Río Santiago 27, Col. Sánchez Ibarra, Tepic, Nayarit, Mexico

[5]Instituto Tecnológico Nacional de México, campus Bahía de Banderas. Crucero a Punta de Mita S/N, Bahía Banderas, Nayarit, Mexico

[6]Centro Regional de Investigaciones Pesqueras Mazatlán. Calzada Sábalo-Cerritos, S/N, Mazatlán, Sinaloa, Mexico

[7]Instituto de Ciencias del Mar y Limnología, Universidad Nacional Autónoma de México. Av. Joel Montes Camarena s/n, Mazatlán, Sinaloa, Mexico

**Correspondence**

This article has been accepted for publication and undergone full peer review but has not been through the copyediting, typesetting, pagination and proofreading process which may lead to differences between this version and the Version of Record. Please cite this article as doi: 10.1111/jfb.14100

F. Amezcua, Instituto de Ciencias del Mar y Limnología, Universidad Nacional Autónoma de México. Av. Joel Montes Camarena s/n, Mazatlán 82040, Sinaloa, Mexico

Email: famezcua@ola.icmyl.unam.mx

**Funding information**

Funding for this research was provided by the project PAPIIT-IG201215, the Slim-WWF foundation and the Western Division of the American Fisheries Society.

ABSTRACT

The age of 296 juvenile scalloped hammerhead sharks *Sphyrna lewini* caught by several fisheries in the Mexican Pacific Ocean from March 2007 to September 2017 were estimated from growth-band counts in thin-sectioned vertebrae. Marginal-increment analysis (MIA) and centrum-edge analysis (CEA) were used to verify the periodicity of formation of the growth bands, whereas elemental profiles obtained from LA-ICP-MS transect scans in vertebrae of 15 juveniles were used as an alternative approach to verify the age in the species for the first time. Age estimates ranged from 0 to 10+ years (42–158.7 cm total length; $L_T$). The index of average percentage error ($I_{APE}$ 3.6%), CV (5.2%), bias plots and Bowker's tests of symmetry showed precise and low-biased age estimation. Both MIA and CEA indicated that in the vertebrae of juvenile *S. lewini* a single translucent growth band was formed during winter (November–March) and an opaque band during summer (July–September), a period of faster growth apparently correlated with a higher sea surface temperature. Peaks in vertebral P and Mn content spatially corresponded with the annual banding pattern in most of the samples, displaying 1.19 and 0.88 peaks per opaque band, respectively, which closely

matched the annual deposition rate observed in this study. Although the periodicity of growth-band formation needs to be verified for all sizes and ages representing the population of the species in the region, this demonstration of the annual formation of the growth bands in the vertebrae of juveniles should lead to re-estimation of growth parameters and productivity to ensure that the population is harvested at sustainable levels.

**KEYWORDS**

centrum-edge and marginal-increment analysis, temperature, growth-band periodicity, vertebra microchemistry

## 1 | INTRODUCTION

The scalloped hammerhead shark *Sphyrna lewini* (Griffith & Smith 1834), is a large and highly migratory circumtropical species found in both coastal and oceanic waters (Compagno, 1984). In the eastern Pacific Ocean, this species ranges from southern California southward to Ecuador (Castro, 2011), where it is heavily harvested since it is frequently captured as target or by-catch in several fisheries. Young-of-the-year and juvenile individuals are captured with artisanal gillnets, bottom longlines and trawl nets in nearshore waters, whereas adults are mainly captured offshore with pelagic longlines (Kotas *et al.*, 2014; Coiraton *et al.*, 2017). Like most elasmobranchs, the species is susceptible to overfishing because of its slow growth, low fecundity, late age of maturity and the association of its

reproductive cycle with coastal areas (Piercy *et al.*, 2007; Torres-Huerta *et al.*, 2008). Furthermore, its specialised traits and complex mating, feeding and predator behaviours (Irschick *et al.*, 2005) have increased its vulnerability and hampered efforts at conservation (Gallagher *et al.*, 2014). It has been categorised as Endangered by the IUCN (Baum *et al.*, 2007).

Knowledge of the age structure and growth rate of a population is required for population models that estimate the productivity of a stock and demonstrate whether a species is harvested at sustainable levels (Cortés, 2000). Studies of age and growth of *S. lewini* around the world (Branstetter, 1987a; Chen *et al.*, 1990; Piercy *et al.*, 2007; Harry *et al.*, 2011; Kotas *et al.*, 2011; Drew *et al.*, 2015) have included Mexico (Anislado-Tolentino & Robinson-Mendoza, 2001; Anislado-Tolentino *et al.*, 2008) but no consensus has been achieved regarding the growth pattern of the species. Some authors (Branstetter, 1987a; Piercy *et al.*, 2007; Harry *et al.*, 2011; Kotas *et al.*, 2011) have suggested an annual formation of the growth bands in the vertebrae, whereas others (Chen *et al.*, 1990; Anislado-Tolentino & Robinson-Mendoza, 2001; Anislado-Tolentino *et al.*, 2008) have suggested that two growth band pairs are formed each year. As yet, no complete age validation and verification have been achieved. It is unclear whether such differences result from the method used, the widely variable sample size per month in each study or the existence of differing patterns of growth for the different stocks and age groups. Since population assessment and management are greatly affected by growth estimates (Cailliet *et al.*, 1986; Campana, 2001), erroneous age estimates of *S. lewini* can lead to inaccurate estimation of its resilience to fishing pressure (Beamish & McFarlane, 1983; Campana, 2001).

Age validation requires proof that growth bands are predictably deposited in the vertebrae. The process of evaluating growth-band deposition in sharks can be categorised into the terms verification and validation (Cailliet, 1990; Cailliet & Goldman, 2004). Verification is defined as "confirming an age estimate by comparison with other indeterminate methods," and validation as "proving the accuracy of age estimates by comparison with a determinate method" (Cailliet, 1990; Cailliet & Goldman, 2004). Because absolute age is only validated when the periodicity of growth-band formation has been validated for all available age classes (Beamish & McFarlane, 1983; Cailliet, 1990; Campana, 2001), this process has often proven difficult when recapture of wild specimens is required (Cailliet & Goldman, 2004), so it is the periodicity of growth-band formation for which validation is typically attempted. For this, centrum-edge analysis (CEA) and marginal-increment analysis (MIA) are the methods most frequently employed for elasmobranchs. However, these have often been hampered by small sample sizes across the species size ranges during incomplete annual periods and by the difficulty in objectively identifying growth bands in the vertebrae of some species (Cailliet *et al.*, 1986). Interpretation is also hindered by lack of discrimination between annual and biannual cycles (Okamura *et al.*, 2013). Hence, new simple and flexible approaches that directly account for periodicity have been developed to improve the accuracy and robustness of MIA (Okamura *et al.*, 2013) and CEA (Okamura & Semba, 2009).

As an alternative approach, microchemical analysis of vertebrae has also been used to validate the periodicity of growth-band formation in vertebrae of elasmobranchs because changes in the concentration of elements such as calcium (Ca) and phosphorus (P) can be related with growth-band deposition or seasons (Jones & Geen, 1977; Cailliet *et al.*, 1986;

Cailliet & Radtke, 1987; Hale *et al.*, 2006; Mohan *et al.*, 2018). Variations in other element concentrations that are related to environmental variables such manganese (Mn) with temperature (Smith *et al.*, 2013) and strontium (Sr) with salinity (Tillett *et al.*, 2011; Scharer *et al.*, 2012) can show a marked seasonality and also prove useful for validating ages (Raoult *et al.*, 2016). This approach can complement the more traditional techniques (Cailliet *et al.*, 1986) and is ideal for endangered species for which samples are few (Goldman *et al.*, 2012; Scharer *et al.*, 2012), or for species with few or no visible growth bands (Raoult *et al.*, 2016).

The aim of the present study was to provide new information on the periodicity of growth-band formation of *S. lewini* in the south-eastern Gulf of California, Mexico, using MIA and CEA methods, together with the approaches developed by Okamura & Semba (2009) and Okamura *et al.* (2013) to improve the accuracy of the age estimations and verify the timing and frequency of the growth-band formation. Age estimates based upon visual growth-band counts were also compared for the first time for this species with the analysis of time-resolved elemental profiles (Ca, P and Mn) in its vertebrae as a complementary approach to verify the periodicity of the formation of growth bands.

## 2 | MATERIAL AND METHODS

### 2.1 | Sample collection

Vertebrae were obtained opportunistically from specimens captured between March 2007 and September 2017 in small-scale and industrial fisheries, landed in several locations of the

south-eastern Gulf of California in the states of Sinaloa (Las Lajitas, La Reforma, Marmól, Mazatlán, Chametla, Teacapán) and Nayarit (Cuautla, Isla Isabel, Boca de Camichín, San Blas, Punta Santa Cruz, Chacala and Bahía Banderas), Mexico (Figure 1). Additional samples were obtained from the shrimp trawl fishery that operates off southern Sinaloa and northern Nayarit (Figure 1). Fishing used surface and bottom gillnets, surface longlines and bottom trawls. Fisheries targeting sharks are prohibited during May to July in the Mexican Pacific Ocean to protect the main reproductive season and the few specimens obtained during this period were incidentally caught by the shrimp trawl and Pacific sierra gillnet fisheries. Sex, total length ($L_T$) and interdorsal length ($L_{ID}$; *i.e.*, distance between the two dorsal-fin insertions) were recorded for each specimen. A set of 10 postcephalic vertebrae was removed, stored on ice and later frozen until preparation for ageing and elemental analyses. $L_T$ was measured to the nearest cm with the tail in the natural position, without depressing it to be in line with the body axis. Estimation of $L_T$ of commercially processed specimens (*i.e.* trunks) used $L_{ID}$ measurement: $L_T = 3.4084L_{ID} + 16.528$ ($n = 71$, $r^2 = 0.97$; Coiraton *et al.*, 2017) and $L_T = 3.402L_{ID} + 16.327$ ($n = 100$, $R^2 = 0.90$; Gallegos-Camacho & Tovar-Ávila, 2011). Because of the difficulties in obtaining adequate sample sizes of adults (8 females and 16 males), the present study focused on immature specimens, of $L_T$ below the estimated size at maturity in the region ($L_{T\,female} < 207$ cm and $L_{Tmale} < 170$ cm; Anislado-Tolentino & Robinson-Mendoza, 2001; Torres-Huerta *et al.*, 2008).

**2.2 | Preparation of vertebrae for ageing**

Following standard protocols (Cailliet & Goldman, 2004), after vertebrae had been defrosted and the neural arch and extraneous tissue removed, individual centra were soaked in 30% $H_2O_2$ to remove remaining tissue, thoroughly rinsed, air dried, mounted on wooden holders and later cut into 0.4 mm sagittal sections with a Buehler low-speed Isomet saw (www.buehler.co.uk).

**2.3 | Age estimation**

The terminology for vertebrae recommended by Cailliet & Goldman (2004) is used throughout the text (Figure 2). Vertebra sections were examined under transmitted light using a binocular dissecting microscope (Zeiss Stemi 508; www.zeiss.com) equipped with a digital camera (Zeiss AxioCam ERc5s) and software (Zen 2.3 Blue Edition; Zeiss). The birthmark was identified as the first translucent band closest to the focus of the vertebra and a change in angle along the corpus calcareum interface; this represented age 0. Each subsequent translucent growth band that extended across both sides of the corpus calcareum was counted (Goldman, 2005). Each vertebra section was read by two readers, with the two readings being at different times. Each count was made with no knowledge of the previous count, or of the sex or size of the shark. When counts differed between the two readings, these sections were re-examined by each reader and a consensus was decided. If disagreement persisted, then those samples were excluded from the analyses. Vertebra centrum radius ($R_V$) was measured as a straight line from the centrum focus to the outer margin of the corpus calcareum to the finest scale possible (Goldman *et al.*, 2012). Linear regression was used to determine the

relationship between $R_V$ and $L_T$. To confirm correct identification of the birthmark, length at the formation of the supposed birthmark was back-calculated by the Fraser–Lee method (Francis, 1990): $L_t = [(R_T)(R_V)^{-1}](L_C - a) + a$, where $L_t$ is the back-calculated length corresponding to age *t*, $R_t$ the distance between the focus and each translucent band at age *t*, $R_V$ the centrum radius, $L_C$ the length at the time of capture and *a* is the intercept of the regression between $R_V$ and $L_C$. Whenever back-calculated length at birth differed from the reported lengths at birth of *S. lewini* in the area of study, the sections were re-examined for the birthmark position by both readers. Those samples where disagreement on the birthmark position persisted were excluded from analysis because of the risk of incorrectly assigning age 0. It is well established that in the south-eastern Gulf of California, pregnant *S. lewini* give birth during the summer months, between May and July (Torres-Huerta et al., 2008), with the formation of the vertebral birthmark deposited at that moment being representative of the transition from an *in-utero* to a *post-partum* life history (Cailliet & Goldman, 2004). Considering that the first translucent band is possibly formed during the following winter months (Piercy et al., 2007; Kotas et al., 2011), the first vertebral growth-band pair of *S. lewini* would therefore represent less than 1 year (8–11 months of age) once such translucent bands are fully formed. However, for the purposes of this study, it was assumed that the first growth-band pair represented a complete year of growth to simplify the age estimates and comparisons with previous studies. It was also considered that such assumption would not affect the precision, bias and verifications process of the periodicity of the growth-band formation because the analyses performed (*i.e.* MIA and CEA) are independent of the estimated age and the duration of the first growth-band formation. It would be however

necessary to determine in the future if considering the first growth band as a full year or estimating the fraction that it would represent could affect the estimation of the population growth parameters.

### 2.4 | Ageing precision and bias

Precision, defined as the reproducibility of repeated measurements on a given structure, was estimated through the traditional index of average percentage error ($I_{APE}$; Beamish & Fournier, 1981): $I_{APE} = \frac{1}{n}\sum_{j=1}^{n}\left[\frac{1}{r}\sum_{i=1}^{r}\frac{|x_{ij}-x_j|}{x_j}\right]$, where $n$ is the number of sharks aged, $r$ is the number of readings, $x_{ij}$ is the $i$th age estimation of the $j$th shark at the $i$th reading and $x_j$ is the mean age calculated for the $j$th shark.

The CV was also used as a precision measure because it has been described as statistically more rigorous and flexible (Chang, 1982): $CVj = [\sqrt{\sum_{i=1}^{R}(x_{ij} - x_j)^2(R-1)^{-1}]x_j^{-1}}$, where $CV_j$ is the age precision estimate for the $j$th fish. This can be averaged across sharks to produce a mean CV. An age-bias plot compared the bias of growth-band counts between the two readers (Campana *et al.*, 1995) and Bowker's test of symmetry (1948) determined whether differences between readers were systematic or due to random error (Hoenig *et al.*,1995): $\chi^2 = \sum_{i=1}^{m-1}\sum_{j=i+1}^{m} \quad [(n_{ij} - n_{ji})^2(n_{ij} - n_{ji})^{-1}]$ where $n$ is the observed frequency in the $i$th row and $j$th column and $nij$ is the observed frequency in the $j$th row and $i$th column.

### 2.5 | Validation of the periodicity of growth-band formation

MIA, as a first validation method, determined the periodicity of the translucent growth-band formation. Marginal increment ratios ($R_{MI}$) were derived (Branstetter & Musick, 1994; Natanson *et al.,* 1995): $R_{MI} - (R_V - R_n)(R_n - R_{n-1})^{-1}$, where $R_V$ is the vertebra centrum radius, $R_n$ is the radius of the last complete translucent band and $R_{n-1}$ is the radius of the penultimate complete translucent band. All measurements were made along the corpus calcareum using digital photographs and software (Zen 2.3 Blue Edition). Individuals of age 0 (young-of-the-year) were excluded from MIA because they have no fully formed winter translucent increments. Monthly averaged $R_{MI}$ values were plotted to detect trends in the growth-band formation. A one-way Kruskal-Wallis test assessed differences in $R_{MI}$ by month and compared the results with previous studies. Following Okamura *et al.* (2013), a circular-linear regression model with random effects was used to adjust three models of growth periodicity (acyclic, annual and biannual cycle) to the $R_{MI}$ data. The Akaike information criterion (AIC; Akaike, 1973) determined which growth cycle best fitted the data.

CEA, as the second validation method, compared the monthly frequencies of translucent and opaque centrum edges. Again, young-of-the-year that only displayed birthmarks were excluded because translucent birthmark periodicity differs from normal growth-band pairs and does not reflect growth seasonality. Following Okamura & Semba (2009), the data were adjusted to different periodicity models (acyclic, annual or biannual), which were compared with AIC to determine which best fit the data. Models were fitted to $R_{MI}$ and CEA data using R software (www.r-project.org), ADMB platform (Fournier *et al.*,

2012; www.admb-project.org) and the program code available in Okamura *et al.,* (2013) and online (http://cse.fra.affrc.go.jp/okamura/program/agevalid/index.html; Okamura & Semba, 2009).

$R_{MI}$ and CEA data were related to the monthly averaged sea surface temperature (SST) registered across the study area by the Coastwatch West Coast Regional Node of the National Oceanic and Atmospheric Administration (www.coastwatch.pfeg.noaa.gov) for the years and months in which $R_{MI}$ and CEA data were available. Pearson's correlation analysis determined whether vertebral growth was influenced by SST.

**2.6 | Elemental profile analysis**

Elemental profiles were analysed in a subset of vertebral sections as an attempt to verify the age estimates obtained by the traditional approaches. Vertebral sections were hand polished with a series of progressively finer grades of lapping paper until the growth bands were clearly visible, sonicated in Milli-Q water (Merck; www.merckmillipore.com) to remove surface contaminants, triple rinsed, dried for 24 h and randomly affixed to acid-washed petrographic slides (subsequently referred to as master slides). One vertebra section from each specimen was used for analyses as it was shown that elemental signatures of *S. lewini* did not differ among vertebrae from the same shark (Schroeder, 2011; Smith et al., 2016). All cleaning and drying procedures were performed under a class-100 laminar-flow clean hood using trace-metal-grade reagents, non-metallic instruments and $HNO_3$ acid-washed glass slides.

A Photon-Machines Analyte.193 excimer UV laser ablation system (LA; LightMachinery; www.lightmachinery.com), connected to an Agilent Technologies 7500CX (www.agilent.com) quadrupole inductively coupled plasma–mass spectrometer (ICP-MS), was employed to characterise the elemental profiles in the vertebrae of *S. lewini*, which were assayed along transects encompassing the area from the focus towards vertebral edge completely within the corpus calcareum (Figure 2). Transects were pre-ablated prior to data acquisition in order to remove possible external contamination. Pre-ablation transect scan speed was 108 μm $s^{-1}$, with a repetition rate of 2 Hz and a spot size of 108 μm. For data acquisition, ablation transect scan speed was 10 μm $s^{-1}$, with a repetition rate of 10 Hz and a spot size of 83 μm.

Data were acquired by the ICP-MS which employed Agilent Technologies ChemStation software operating in time-resolved analysis mode to collect raw data of the ion count rates in counts per second ($c$ $s^{-1}$) for $^{31}P$, $^{43}Ca$ and $^{55}Mn$ along the vertebral transects. As there is no matrix-matched standard available for shark vertebrae, NIST-612 silicate glass served as external calibration reference material (values given in Pearce *et al.*, 1997) and was ablated with two replicates before and after every fifth vertebral section was sampled. MACS-3 microanalytical carbonate standard material (Koenig & Wilson, 2007) was ablated in brackets before and after each master slide to estimate experiment-wide levels of precision. Raw $c$ $s^{-1}$ data for $^{31}P$ and $^{55}Mn$ were standardised to the number of $^{43}Ca$ ions ($c$ $s^{-1}$) obtained simultaneously in the structure by deriving element-to-Ca $c$ $s^{-1}$ data ratios (element:Ca) to adjust for variability in instrument sensitivity and the amount of ablated material and to provide accurate data on the relative distribution of the target elements along the transect

accounting for potential differences in $^{43}Ca$ data within the vertebrae, which have been reported to occur between opaque and translucent growth bands for some species (*e.g.* Scharer *et al.*, 2012; Raoult *et al.*, 2016; Mohan *et al.*, 2018). Background data corresponding to gas blanks were collected for 90 s before and after each transect was ablated. Parsing, processing and quality control of the raw *c* $s^{-1}$ data generated by the methods described above were performed using the free download Fathom Toolbox for Matlab™ (Jones, 2017).

Data of the $^{43}Ca$ raw ion count rates (*c* $s^{-1}$) and the $^{31}P$:$^{43}Ca$ and $^{55}Mn$:$^{43}Ca$ *c* $s^{-1}$ data ratios were plotted *v.* vertebral transect distance (μm) for each sample. An 11 point running average window size was applied to filter–smooth the data, reduce the noise and aid in identifying the underlying pattern of the elemental profiles (Sinclair *et al.*, 1998). The degree to which smoothed peaks above the background noise in elemental profiles corresponded to opaque bands was evaluated by overlaying the position of opaque bands on plots obtained by measuring the distance (μm) from the focus to the mid-point of each opaque band of the vertebra. Linear regression analyses investigated how well the opaque growth-band counts (independent variable) predicted peaks (dependent variables) in the $^{31}P$:Ca, $^{55}Mn$:Ca and $^{43}Ca$ transect profiles.

All data were assessed for normality and homogeneity of variances by Shapiro-Wilk's and Levene's tests before the statistical analyses. When required, data were $\log_{10}$-transformed to conform to the assumptions of parametric analyses.

## 3 | RESULTS

### 3.1 |Age estimation

Overall, the vertebrae from 296 young-of-the-year and juvenile specimens of *S. lewini* from the south-eastern Gulf of California were analysed: 135 females (47.3–193 cm $L_T$) and 161 males (42–158.7 cm $L_T$; Figure 3a). Growth bands were relatively easy to discern in all vertebral sections except for those in *S. lewini* < 2 years old. Excluding the pre-birth and birthmarks, the number of translucent growth bands counted along the corpus calcareum (and thus the estimated ages) ranged from 0 to 10+ years for females and 0 to 7+ years for males (Figure 3b). $R_V$ and $L_T$ were strongly correlated, with a linear relationship ($L_T = 17.35R_V + 14.52$, $r^2 = 0.92$; $P < 0.05$). Back-calculated length at the formation of the birthmark, $L_T$, ranged from 46.6 to 65.7 cm (mean ± SD = 53.8± 3.3 cm).

### 3.2 | Ageing precision

The $I_{APE}$ and CV between the final counts of the two readers (4.3% and 6.1% respectively) indicated a high precision of growth-band counts. Most of the counts agreed exactly between readers (84.4%) and 98.4% within one band pair. In addition, the age-bias plot (Figure 4) and Bowker's test of symmetry showed no systematic bias and low disagreement between readers ($\chi^2 = 8.12$, df 8, $P < 0.5$).

### 3.3 | Validation of the periodicity of growth-band formation

In total, 235 specimens of *S. lewini* were suitable for MIA and CEA. Despite low sample sizes in May ($n$ = 2), June ($n$ = 1), July ($n$ = 2) and December ($n$ = 6), the $R_{MI}$ data differed significantly among months (Kruskal–Wallis $\chi^2$= 60.02, $P < 0.001$); a trend to increase in June and to decline in October suggested that a single translucent growth band was formed between November and March (Figure 5a). AIC values obtained with the Okamura *et al.* (2013) method (87.07 for acyclic model, 57.37 for annual and 95.85 for biannual cycle models) supported an annual cycle of growth-band formation. The trend was positively correlated with the annual variation pattern of the averaged SST (Pearson's correlation: $r$ = 0.74; $P < 0.01$; Figure 5a), indicating that vertebral growth of *S. lewini* is probably strongly related to SST.

Of the 235 vertebrae considered for CEA, 48.5% had a translucent centrum edge, with the highest frequency occurring in January and the lowest in June and July (Figure 5b). The variation of the monthly proportions of translucent edges was seasonal and closely followed the trend exhibited by the monthly averaged $R_{MI}$ (Figure 5a,b), supporting the hypothesis that a single translucent growth band was formed during the winter months. AIC values obtained with the Okamura & Semba (2009) method (327.6 for acyclic model, 317.1 for annual and 331.4 for biannual models) similarly supported an annual cycle of the growth-band formation in the vertebrae of juveniles of *S. lewini* (Figure 5b). This trend also followed the annual variation pattern of the averaged SST registered in the study area with the highest proportion of translucent edges occurring during the coldest months (22.9–24.5°C) and the lowest proportion when the temperatures were the highest (27–30°C; Pearson's correlation $r$ = 0.67, $P < 0.01$; Figure 5b).

### 3.4 | Elemental profiles analysis

Vertebrae samples from 15 juvenile specimens of *S. lewini* aged from 1 to 5 years (66.4–90.8 cm $L_T$) collected in La Reforma ($n$ = 5), Chametla ($n$ = 5) and Teacapán ($n$ = 5) were made available for the LA-ICP-MS analyses performed as an attempt at age verification (Table 1).

The spatial variation of $^{55}$Mn:Ca along the vertebral transects was significantly correlated with the visible pattern of opaque bands in the samples ($r^2$= 0.48; Figures 6a, 7). The corresponding linear relationship between the number of smoothed peaks identified in the $^{55}$Mn:Ca profile (dependent variable) and the number of opaque growth bands (independent variable) was $y = 0.88x + 0.34$, $P < 0.01$ (Figure 6a). $^{55}$Mn:Ca data accurately predicted the number of opaque growth bands in 66.6% ($n$ = 10) of the vertebrae sampled. For the remaining 5 samples, the number of peaks in the $^{55}$Mn:Ca profiles differed from the number of opaque growth bands by –2 to +2 counts (Figure 6a).

Although the spatial variation of $^{31}$P:Ca along the vertebral transects was also significantly correlated with the visible pattern of opaque bands in the samples ($r^2$ = 0.54) (Figures 6b, 7), $^{31}$P:Ca data could accurately predict the number of opaque growth bands in only 46.6% of the samples ($n$ = 7). For the remaining 8 samples, the number of peaks in the $^{31}$P:Ca profiles differed from the number of opaque growth bands by –1 to +4 counts. The corresponding linear relationship was $y = 1.19x + 0.19$, $P < 0.01$ (Figure 6b).

The $^{43}$Ca profiles did not exhibit a consistent pattern among individuals. $^{43}$Ca values either showed a progressive increase from the focus to the edge ($n$ = 6), a progressive decline

from the focus to the edge ($n$ = 3; Figure 7), or a constant pattern along the transects profiles ($n$ = 6). The predictions of the $^{43}$Ca data were highly variable ($r^2$ = 0.1, $P$ > 0.5) and thus are not presented here (Table 1).

## 4 | DISCUSSION

### 4.1 | Age estimations

There is no *a priori* value of precision that can be designated as a target for ageing studies, since precision is highly influenced not only by the species biology but also by the age reader (Campana, 2001). However, a review (Campana, 2001) of 131 ageing papers stated that all studies that have estimated the age of sharks based on vertebral growth-band counts reported CV precision values > 10%. On that basis, Campana (2001) recommended that ageing studies be carried out with a CV of < 7.6%, corresponding to an $I_{APE}$ of 5.5%, serving as a reference point. Accordingly, the CV value obtained in this study (6.1%) was consistent with a precise age estimation, especially since CV values as low as 6.8% (Drew *et al.*, 2015) and as high as 17.9% (Harry *et al.*, 2011) have been reported in studies of *S. lewini* elsewhere. In addition, the $I_{APE}$ value obtained here (4.3%) was also consistent with those obtained from previous ageing studies of *S. lewini* (3.2%, Piercy *et al.*, 2007; 3.7%, Anislado-Tolentino *et al.*, 2008; 5.6%, Kotas *et al.*, 2011), a further indication of a precise age estimation with low bias.

The validation of the first increment is mandatory in ageing studies because without a correctly defined starting point age estimations would be consistently biased, especially when

the goal of a study is to validate the periodicity of the growth-band formation rather than the absolute age, as chemical tagging studies do (Campana, 2001). According to the length-at-birth of *S. lewini* reported in the southeastern Gulf of California (41–53 cm $L_T$; Anislado-Tolentino, 2000; Torres-Huerta *et al.*, 2008, Coiraton *et al.*, 2017), the back-calculated length at birth obtained in the present study (53.8 ± 3.3 cm, mean ± SD) indicated that the birthmark was correctly discerned by readers in all vertebral sections.

### 4.2 | Validation of the periodicity of growth-band formation

Age estimates derived from visual counts of concentric growth zones in calcified structures such as vertebrae rely on validating the temporal periodicity of formation of these zones over the lifespan of the species (Beamish & McFarlane, 1983; Cailliet *et al.*, 1986; Campana, 2001). Although validation of the periodicity of growth-band formation in vertebrae of *S. lewini* was attempted in previous studies (Branstetter, 1987a; Anislado-Tolentino & Robinson-Mendoza, 2001; Anislado-Tolentino *et al.*, 2008; Harry *et al.*, 2011; Drew *et al.*, 2015), few have provided conclusive results; the use of a single method of validation (either MIA or CEA) precluded an objective comparison of results, samples and ages were lacking for some months and there was a mixture of individuals of different sizes and ages (in some cases even young-of-the-year). It is important to separate the life stages in *S. lewini* ageing studies to avoid sex and life-stage bias, since these can be subject to different growth patterns (Campana, 2001).

In this study, only immature specimens were considered because of the difficulties in obtaining adequate sample sizes of all life stages forming the population. The MIA and CEA methods were combined as a validation process and results indicated that in the Mexican Pacific Ocean a single translucent growth band was formed in the vertebrae of the juveniles during the winter months (November–March), a period of slower growth. A single opaque growth band was formed during the summer months, between June and September, a period of faster growth. A similar pattern of growth has been reported for *S. lewini* in the north-western Atlantic Ocean and Gulf of Mexico (Piercy *et al.*, 2007; Branstetter, 1987a), southern Brazil (Kotas *et al.*, 2011), eastern Australia (Harry *et al.*, 2011) and Indonesia (Drew *et al.*, 2015).

Although MIA was inconclusive for elucidating the periodicity of growth-band formation in the vertebrae of *S. lewini* in previous studies (Drew *et al.*, 2015), here it allowed visual discernment of a trend in the monthly $R_{MI}$ data in spite of the low sample size in some months. This observation was statistically supported by a Kruskal-Wallis test and the model developed by Okamura *et al.* (2013), which provided strong evidence for an annual growth cycle for $R_{MI}$ data. Burnham & Anderson (2002) suggested that a difference of > 2 in AIC values should be required to identify with certainty the best model in terms of the Kullback–Leibler divergence. Here, the annual cycle model had an AIC difference of > 10, confirming that this model was the best fitted to the $R_{MI}$ data. Moreover, CEA also graphically revealed a contrast of growth between the winter (higher proportions of translucent edges) and summer (higher proportions of opaque edges) in spite of the lack of data between May and July and the predictions of the annual cycle model developed by Okamura & Semba (2009) clearly

showed this trend. This model is applicable to data sets that lack data for some months (Okamura & Semba, 2009), as in the present study.

Evidence of latitudinal variations in growth have been found for various species of elasmobranchs (Driggers *et al.*, 2004; Licandeo & Cerna, 2007), including other hammerhead sharks such as *Sphyrna tiburo* (L. 1758) (Lombardi-Carlson *et al.*, 2003). Those variations could be occurring also for *S. lewini* among geographical regions (*e.g.*, Taiwan; Chen *et al.*, 1990). Although this hypothesis must be tested, the assumption of the existence of different patterns of growth within the Mexican Pacific Ocean (Anislado-Tolentino & Robinson-Mendoza, 2001; Anislado-Tolentino *et al.*, 2008) seems unlikely for *S. lewini*. The observed differences among studies may be due in part to differences in the vertebra preparation and growth-band interpretation. The annual formation of growth bands in vertebrae of two other *Sphyrna* species, *Sphyrna mokarran* (Rüppell 1837) (Passerotti *et al.*, 2010,) and *S. tiburo* (Parsons, 1993; Carlson & Parsons, 1997) have been directly validated by bomb radiocarbon and chemical tagging in vertebrae, which gives support to the findings of the present study and those of the earlier ones that also supported an annual growth cycle for *S. lewini* in other regions of the world. Considerable progress has been made in age validation efforts since the results of Chen *et al.* (1990), Anislado-Tolentino & Robinson-Mendoza (2001) and Anislado-Tolentino *et al.* (2008) were published and the particularly robust and statistically rigorous methods developed by Okamura & Semba (2009) and Okamura *et al.* (2013) were not available at the time to facilitate the verification process of the periodicity of growth-band formation. Here, the use of such approaches addressed this uncertainty for *S. lewini* in the Mexican Pacific Ocean, even though only juveniles could be assessed. It is still necessary to

verify the timing and frequency of the growth-band formation in the vertebrae of adult specimens across the area, because growth can change once individuals mature (Wells *et al.*, 2013; Kinney *et al.*, 2016). Although the periodicity of growth-band formation needs to be validated for all sizes and ages representing the population of the species in the region, the annual formation of the growth bands in the vertebrae of juveniles makes it necessary to re-estimate growth parameters and productivity to ensure that the population is harvested at sustainable levels.

Banding patterns in vertebrae of elasmobranchs may be related to growth in size rather than age (Natanson & Cailliet, 1990; Natanson *et al.*, 2008; Baremore *et al.*, 2009). The fact that some species do not show an annual banding pattern [*e.g.*, basking shark *Cetorhinus maximus Cetorhinus maximus* (Gunnerus 1765) (Natanson *et al.*, 2008)] or exhibit ontogenetic changes in their growth cycle over the life history [*e.g.*, shortfin mako *Isurus oxyrinchus* Rafinesque 1810 (Wells *et al.*, 2013; Kinney *et al.*, 2016)] reinforces the need to confirm the temporal meaning of these growth increments for each species (Natanson, 1993). Seasonal changes in temperature, light and food availability or migrations, may cause the deposition of periodic growth bands in the vertebrae of elasmobranchs (Pratt & Casey, 1983; Branstetter, 1987b), although causes can vary depending on the species. *S. lewini* is a large and migratory species that cannot be maintained in captivity to conduct controlled experiments and explore those cues. However, it appeared that seasonal variations in temperature influenced in part its vertebral growth rate and banding pattern in the Mexican Pacific Ocean. The highest temperatures that occurred during the summer months were related to the highest growth increments and opaque band formation at the edge of these shark vertebrae. Similar results were also observed for *I. oxyrinchus* (Ribot-Carballal *et al.*, 2005) and recent experimental studies have shown that increased temperatures had a positive effect on the mean growth rates of the round stingray *Urobatis halleri*(Cooper 1863) (Smith *et al.*, 2013), although the most elevated growth rates were

found for specimens that had overall experienced the least amount of change in temperature and the other variables (Smith *et al.*, 2013). Although the apparent relationship that relates vertebral growth and seawater temperature allowed to verify the annual cycle of growth bands of juvenile *S. lewini* in the Mexican Pacific Ocean, the forecasted end-of-century increases in temperature might also have detrimental effects on these sharks (Pistevos et al., 2015). Recent experiments showed that more elevated temperatures increased food intake and energetic demand which, when combined with elevated $CO_2$, could also affect the hunting behaviour of sharks (Pistevos et al., 2015). Even though investigating the effects of the global warming on *S. lewini* was not the purpose of this study, these are of concern and need to be investigated in the near-future.

### 4.3 | Elemental profile analysis

Analyses of elemental profiles ($^{43}$Ca, $^{31}$P and $^{55}$Mn) in vertebrae of juvenile specimens of *S. lewini* were used in this study as an attempt to verify for the first time the periodicity of the growth-band formation and age estimates derived from visual counts of the opaque growth bands by matching peaks in elemental concentrations with the seasonal banding pattern. The use of strontium ($^{88}$Sr) was not explored for *S. lewini* because little is known about the age-related movement patterns of this species (Harry *et al.*, 2011; Ketchum *et al.*, 2014) and seawater chemistry was not available to compare with the variations of Sr in its vertebrae.

No significant relationship was found between peaks in $^{43}$Ca profiles and the opaque growth bands but the peaks in $^{31}$P:Ca and $^{55}$Mn:Ca spatially corresponded with the annual banding pattern in most of the samples. $^{31}$P:Ca profiles displayed 1.19 peak per opaque band while $^{55}$Mn:Ca displayed 0.88 peak per opaque band; this closely matched the annual

deposition rate in juveniles obtained from the verification analyses of this and previous studies (Branstetter, 1987a; Piercy *et al.*, 2007; Harry *et al.*, 2011; Kotas *et al.*, 2011). However, these interpretations remain tentative because age estimates explained only half of the variability of the elemental patterns, as shown by the low, but significant, correlation coefficients. When $^{31}$P:Ca and $^{55}$Mn:Ca data could not accurately predict the number of opaque growth bands, the predictions did not vary in a predictable manner and could be both less than or greater than opaque band counts; this indicates that the incorporation of these elements in the vertebrae of *S. lewini* might be mediated by factors other than growth, which perhaps do not show any temporal cycle.

Several authors have explored the elemental variations (*e.g.* Ca, P, Sr, Mn) in vertebrae of elasmobranchs as they can relate to growth-band deposition (Jones & Geen, 1977; Cailliet & Radtke, 1987; Hale *et al.*, 2006; Scharer *et al.*, 2012; Raoult *et al.*, 2016; Mohan *et al.*, 2018). Ca was not useful for verifying ages in most of the species [*Pristis pectinata* Latham 1794, *Carcharodon Carcharias* (L. 1758), *Sphyrna zygaena*(L. 1758), *Heterodontus portusjacksoni* (Meyer 1793), *Carcharhinus obscurus* (LeSueur 1818), *Carcharhinus brevipinna* (Valenciennes 1839), *Prionace glauca*(L. 1758), *Alopias vulpinus* (Bonnaterre 1788) and *I. oxyrinchus* (Scharer *et al.*, 2012; Raoult *et al.*, 2016; Mohan *et al.*, 2018)], although the variations of Ca were strongly related with opaque growth bands in the vertebrae of *U. halleri* and spiny dogfish *Squalus acanthias* L. 1758 (Jones & Geen, 1977; Hale *et al.*, 2006). Raoult *et al.* (2016) stated that a stronger correlation might be found if more individuals of these species were analysed but the results of the present study, as in previous studies (Scharer *et al.*, 2012; Raoult *et al.*, 2016; Mohan *et al.*, 2018), showed

that banding pattern in vertebrae of elasmobranchs may be more closely related to element absorption than to calcification or growth. One explanation for the discrepancy observed among the elemental patterns in vertebrae of these various elasmobranch species is that they exhibit contrasting patterns of dispersion that have possibly impeded interpretation and comparison of the data obtained. The different species occupy different habitats (*i.e.*, coastal, oceanic or both) and vary widely in their elemental patterns, with some elements being more accurate than others for predicting the age estimates of a species.

Variations of $^{31}$P also exhibited a yearly period in the vertebrae of *S. acanthias* (Jones & Geen, 1977), which they concluded was an independent way to estimate age. Hale *et al.* (2006) and Scharer *et al.* (2012) found no apparent relationship of peaks in P in the vertebrae of *P. pectinata* and *U. halleri* with opaque growth bands. In coastal waters, concentrations of P typically exhibit winter maxima and summer minima, thus showing a yearly period of change; Ca is by contrast relatively abundant and remains practically constant year-round (Jones & Geen, 1977). This might explain why Ca has not been useful for verifying the ages of most species.

As in the present study, $^{55}$Mn was the most consistent in accurately predicting the ages of *P. glauca*, *A. vulpinus* and *I. oxyrinchus* (Mohan *et al.*, 2018). Incorporation of $^{55}$Mn in vertebrae is enhanced by a rise in temperature (Smith *et al.*, 2013), as are the growth rates of elasmobranchs (Pistevos *et al.*, 2015). These findings may explain why variations in $^{55}$Mn could be correlated with the number of growth bands, since the species differ in their movement patterns (Sepulveda *et al.*, 2004; Nakano & Stevens, 2008; Cartamil *et al.*, 2010; Wells *et al.*, 2013, 2017). As a coastal and oceanic species, *S. lewini* has complex patterns of

dispersion (Klimley, 1987; Duncan & Holland, 2006; Hoyos-Padilla *et al.,* 2014) and despite extensive studies little is known about the movements of juveniles (Harry *et al.,* 2011; Ketchum *et al.,* 2014). The use of Mn might help to verify the age estimates of juvenile *S. lewini* when combined with other approaches, especially since the vertebral growth rate and banding pattern of these sharks is related to seasonal variation in the SST of the eastern Gulf of California.

All previous studies that have assessed vertebral microchemistry of sharks using LA-ICP-MS analyses used $^{43}$Ca as an internal standard element to standardise the concentration data of the elements of interest because the elemental composition of the hydroxyapatite matrix that constitutes the vertebrae of sharks is dominated by Ca (Urist, 1961; Clement, 1992) and this element was assumed to be homogenously distributed within the vertebrae for most species, being this often quantified in advance as a mean species or family-specific percentage mass of Ca value (%Ca) of the vertebrae (Izzo et al., 2016; Lewis et al., 2016; McMillan et al., 2018; Mohan et al., 2018). The fact that Ca did not exhibit a constant pattern along the vertebral transects of most samples in this study raises a question about the suitability of this element as an internal standard to derive the element:Ca ratios, especially since a precondition for the successful use of an element as internal standard for LA-ICP-MS analyses is that it is homogeneously distributed within the samples (Limbeck et al., 2015). Nevertheless, Ca appears to be the only major element occurring naturally in the vertebrae of sharks that could be optimally used as an internal standard to account for fluctuations in the laser-ablation yield, ensure reliability of the concentration measurements of the elements of interest and allow comparisons among individuals and species. In addition, the fact that the

$^{55}$Mn and $^{31}$P data were standardised to $^{43}$Ca in spite of the apparent spatial heterogeneity of this element within the vertebrae of *S. lewini* probably did not affect the results of this study because $^{43}$Ca was measured simultaneously along the transects (McMillan et al., 2017) rather than being estimated in advance as a mean species-specific %Ca value using solution based ICP-MS (*i.e.*, whole vertebrae) or stoichiometrically calculated, which would have not indicated whether the element was actually homogenously distributed within the structure (Limbeck et al., 2015).

In conclusion, analyses of $^{31}$P and $^{55}$Mn profiles in vertebrae of sharks might help in verifying the banding pattern of species that exhibit seasonal movements among habitats or that are subjected to environmental changes during growth, as in *S. lewini*. It seems necessary, however, to emphasize the importance of standardising the elemental data to the actual number of Ca ions measured simultaneously in the structure in order to obtain accurate element:Ca values that account for potential differences in $^{43}$Ca along the vertebral transects. Since banding patterns in vertebrae of elasmobranchs are also caused by changes in environmental conditions, it is also possible that this method would provide better results when seawater chemistry is available to compare with the patterns observed in the vertebrae and when older specimens can be assessed to fully appreciate the possible cyclical variations of the elements. Reliable interpretation of variations in vertebral elemental patterns to estimate ages of a species would require, however, substantially stronger statistical relationships with the number of opaque growth bands.

**ACKNOWLEDGEMENTS**

The first author thanks the Posgrado en Ciencias del Mar y Limnología, UNAM and CONACyT, Mexico for the support during her graduate studies. David L. Jones and Ernst Peebles provided invaluable support and training in LA-ICP-MS analyses at USF's College of Marine Sciences. Many thanks to G. Alonso-Sosa from Pesca Siglo XXI and all the artisanal fishers for providing samples. The authors also gratefully acknowledge the assistance of A. Valencia, M. Cervantes and E. Armenta Valenzuela with sample preparation and A. Grant with the revision of the language. The manuscript benefited from the contributions of two anonymous referees during the review process. The research presented here partially fulfills requirements for the first author's doctoral degree.

## AUTHOR CONTRIBUTIONS

C.C. and J.T.Á. designed the experiments; C.C., F.A., J.T.Á. and R.G.C. collected the samples; C.C., K.G.G., R.G.C. and D.A.C.A. prepared the samples for analysis; C.C. and K.G.C. read the vertebrae; C.C. performed the LA-ICP-MS experiments; C.C., K.G.C. and J.A.R.M. analysed the data; F.A. contributed reagents, materials and analysis tools; C.C. wrote the paper.

## REFERENCES

Akaike, H. (1973). Maximum likelihood identification of gaussian autoregressive moving average models. *Biometrika, 60*, 255–265.

Anislado-Tolentino, V. (2000). Ecología pesquera del tiburón martillo Sphyrna lewini (Griffith y Smith, 1834) en el litoral del estado de Michoacán, México, Universidad Nacional Autónoma de México, Mexico.

Anislado-Tolentino, V. & Robinson-Mendoza, C. (2001). Edad y crecimiento del tiburón martillo *Sphyrna lewini* (Griffith y Smith, 1834) en el Pacífico central de México. *Ciencias Marinas, 27,* 501–520.

Anislado-Tolentino, V., Cabello Gallardo, M., Amezcua-Linares, F. & Robinson-Mendoza, C. (2008). Age and growth of the scalloped hammerhead shark, *Sphyrna lewini* (Griffith & Smith, 1834) from the southern coast of Sinaloa, Mexico. *Hidrobiologica, 18,* 31–40.

Baremore, I. E., Andrews, K. I. & Hale, L. F. (2009). Difficulties associated with modeling growth in the atlantic angel shark (*Squatina dumeril*). *Fisheries Research, 99,* 203–209.

Baum, J., Clark, S., Domingo, A., Ducrocq, M., Lamónaca, A. F., Gaibor, N., Graham, R., Jorgensen, S., Kotas, J. E., Medina, E., Martinez-Ortiz, J., Monzini Taccone di Sitizano, J., Morales, M. R., Navarro, S. S., Pérez, J. C., Ruiz, C., Smith, W., Valenti, S. V. & Vooren, C.M. (2007). *Sphyrna lewini.* IUCN 2010. IUCN Red List of Threatened Species. Available at www.iucnredlist.org/details/39385/0 (last accessed 12 June 2018)

Beamish, R. & Fournier, D. (1981). A method for comparing the precision of a set of age determinations. *Canadian Journal of Aquatic Sciences, 38,* 982–983.

Beamish, R. & McFarlane, G. (1983). The forgotten requirement for age validation in fisheries biology. *Transactions of the American Fisheries Society, 112,* 735–743.

Bowker, A.H. (1948). A test for symmetry in contingency tables. *Journal of the American Statistical Association, 43,* 572-574.

Branstetter, S. (1987a). Age, growth and reproductive biology of the silky shark, *Carcharhinus falciformis* and the scalloped hammerhead, *Sphyrna lewini,* from the northwestern Gulf of Mexico. *Environmental Biology of Fishes, 19,* 161–173.

Branstetter, S. (1987b). Age and growth validation of newborn sharks held in laboratory aquaria, with comments on the life history of the atlantic sharpnose shark, *Rhizoprionodon terraenovae*. *Copeia, 1987,* 291–300.

Branstetter, S. & Musick, J. A. (1994). Age and growth estimates for the sand tiger in the northwestern Atlantic Ocean. *Transactions of the American Fisheries Society, 123*, 242–254.

Burnham, K. P. & Anderson, D. R. (2002). Model Selection and Multimodel Inference: A Practical Information-Theoretic Approach, 2nd edn. New York, NY: Springer.

Cailliet, G. & Goldman, K. (2004). Age Determination and Validation in Chondrichthyan Fishes. In Biology of Sharks and their Relatives (Carrier, J. C., Musick, J. A., Heithaus, M. R., eds), pp. 399–447 Boca Raton, Florida: CRC Press.

Cailliet, G. M. (1990). Elasmobranch age determination and verification: an update review. In Elasmobranchs as Living Resources pp. 157–165.

Cailliet, G. M. & Radtke, R. L. (1987). A progress report on the electron microprobe analysis technique for age determination and verification in elasmobranchs. In Age and

Growth of Fish (Summerfelt, R. C., Hall, G. E., eds), pp. 359–369 Iowa State University Press.

Cailliet, G. M., Radtke, R. L. & Welden, B. A. (1986). Elasmobranch age determination and verification: a review. In Indo-Pacific Fish Biology: Proceedings of the second international conference on Indo-Pacific fishes (Ichthyological Society of Japan, ed), pp. 345–360 Tokyo.

Campana, S., Annand, M. & McMillan, I. (1995). Graphical and statistical methods for determining the consistency of age determinations. *Transactions of the American Fisheries Society, 124*, 131–138.

Campana, S. E. (2001). Accuracy, precision and quality control in age determination, including a review of the use and abuse of age validation methods. *Journal of Fish Biology, 59*, 197–242.

Carlson, J. K. & Parsons, G. R. (1997). Age and growth of the bonnethead shark, *Sphyrna tiburo*, from northwest Florida, with comment on clinal variations. *Environmental Biology of Fishes, 50*, 331–341.

Cartamil, D., Wegner, N. C., Kacev, D., Ben-Aderet, N., Kohin, S. & Graham, J. B. (2010). Movement patterns and nursery habitat of juvenile thresher sharks *Alopias vulpinus* in the Southern California Bight. *Marine Ecology Progress Series, 404*, 249–258.

Castro, J. I. (2011). The hammerhead sharks. In The Sharks of North America pp. 504–531 New York, NY: Oxford University Press.

Chang, W. Y. B. (1982). A statistical method for evaluating the reproducibility of age determination. *Canadian Journal of Fisheries and Aquatic Sciences, 39*, 1208–1210.

Chen, T. C., Leu, T. C., Joung, S. J. & Lo, N. C. H. (1990). Age and growth of the scalloped hammerhead, *Sphyrna lewini*, in the northeastern Taiwan waters. *Pacific Science, 44*, 156–170.

Clement, J. G. (1992). Re-examination of the fine structure of endoskeletal mineralisation in Chondrichthyans: implications for growth, ageing and calcium homeostasis. *Marine and Freshwater Research, 43,* 157–181.

Coiraton, C., Amezcua, F. & Salgado-Ugarte, I. H. (2017). Estructura de longitudes de las capturas del tiburón martillo común (*Sphyrna lewini*) en el Pacífico Mexicano. *Ciencia Pesquera*, *25*, 27–40.

Compagno, L. J. V. (1984). FAO Species Catalogue. Vol. 4. Part 2. Sharks of the World: An Annotated and Illustrated Catalogue of Shark Species Known to Date. *FAO Fisheries Synopsis*, Rome.

Cortés, E. (2000). Life history patterns and correlations in sharks. *Reviews in Fisheries Science, 8,* 299–344.

Drew, M., White, W. T., Dharmadi, Harry, A. V. & Huveneers, C. (2015). Age, growth and maturity of the pelagic thresher *Alopias pelagicus* and the scalloped hammerhead *Sphyrna lewini*. *Journal of Fish Biology, 86,* 333–354.

Driggers, W., Carlson, J., Cullum, B., Dean, J. & Oakley, D. (2004). Age and growth of the blacknose shark, *Carcharhinus acronotus*, in the western North Atlantic Ocean with comments on regional variation in growth rates. *Environmental Biology of Fishes ,71,* 171–178.

Duncan, K. M. & Holland, K. N. (2006). Habitat use, growth rates and dispersal patterns of juvenile scalloped hammerhead sharks *Sphyrna lewini* in a nursery habitat. *Marine Ecology Progress Series, 312,* 211–221.

Fournier, D. A., Skaug, H. J., Ancheta, J., Ianelli, J., Magnusson, A., Maunder, M. N., Nielsen, A. & Sibert, J. (2012). AD Model Builder: using automatic differentiation for statistical inference of highly parameterised complex nonlinear models. *Optimization Methods and Software, 27,* 233–249.

Francis, R. I. C. C. (1990). Back-calculation of fish length: a critical review. *Journal of Fish Biology, 36,* 883–902.

Gallagher, A. J., Hammerschlag, N., Shiffman, D. S. & Giery, S. T. (2014). Evolved for extinction: the cost and conservation implications of specialisation in hammerhead sharks. *BioScience, 64,* 619–624.

Gallegos-Camacho, R. & Tovar-Ávila, J. (2011). Estimación de las longitudes total, furcal y patrón de juveniles de tiburón martillo, *Sphyrna lewini* (Carcharhiniformes: Sphyrnidae), a partir de las longitudes alternativa e interdorsal. *Ciencia Pesquera, 19,* 49–63.

Goldman, K. (2005). Age and growth of elasmobranch fishes. In Management Techniques for Elasmobranch Fisheries (Musick, J. A., Bonfil, R. B., eds), p. 76 Rome: FAO Fisheries Technical Paper.

Goldman, K., Cailliet, G., Andrews, A. & Natanson, L. (2012). Assessing the age and growth of chondrichthyan fishes. In Biology of Sharks and their Relatives (Carrier, J. C., Musick, J. A., Heithaus, M. R., eds), pp. 423–451 Boca Raton, Florida.

Hale, L. F., Dudgeon, J. V., Mason, A. Z. & Lowe, C. G. (2006). Elemental signatures in the vertebral cartilage of the round stingray, *Urobatis halleri*, from Seal Beach, California. *Environmental Biology of Fishes, 77,* 317–325.

Harry, A. V., Macbeth, W. G., Gutteridge, A. N. & Simpfendorfer, C. A. (2011). The life histories of endangered hammerhead sharks (Carcharhiniformes, Sphyrnidae) from the east Coast of Australia. *Journal of Fish Biology, 78,* 2026–2051.

Hoenig, J. M., Morgan, M. J. & Brown, C. A. (1995). Analyzing differences between two age determination methods by tests of symmetry. *Canadian Journal of Aquatic Sciences, 52,* 364–368.

Hoyos-Padilla, E. M., Ketchum, J. T., Klimley, A. P. & Galván-Magaña, F. (2014), Ontogenetic migration of a female scalloped hammerhead shark *Sphyrna le*wini in the Gulf of California. *Animal Biotelemetry, 2,* 17.

Irschick, D., Dyer, L. & Sherry, T. W. (2005). Phylogenetic methodologies for studying specialisation. *Oikos, 110,* 404–408.

Izzo, C., Huveneers, C., Drew, M., Bradshaw, C. J. A., Donnellan, S. C. & Gillanders, B. M. (2016). Vertebral chemistry demonstrates movement and population structure of bronze whaler. *Marine Ecology Progress Series, 556,* 195–207.

Jones, B. C. & Geen, G. H. (1977). Age determination of an elasmobranch (*Squalus acanthias*) by X-Ray spectrometry. *Journal of the Fisheries Research Board of Canada, 34,* 44–48.

Jones, D. L. (2017) The Fathom Toolbox for MATLAB: software for multivariate ecological and oceanographic data analysis. College of Marine Science, University of South

Florida, St. Petersburg, FL, USA. Available from: https://www.marine.usf.edu/research/matlab-resources/ (last accessed 19 April 2019)

Ketchum, J. T., Hearn, A., Klimley, A. P., Espinoza, E., Peñaherrera, C. & Largier, J. L. (2014). Seasonal changes in movements and habitat preferences of the scalloped hammerhead shark (*Sphyrna lewini*) while refuging near an oceanic island. *Marine Biology, 161,* 755–767.

Kinney, M. J., Wells, R. J. D. & Kohin, S. (2016). Oxytetracycline age validation of an adult shortfin mako shark *Isurus oxyrinchus* after 6 years at liberty. *Journal of Fish Biology, 89, 1828–1833.*

Klimley, A. P. (1987). The determinants of sexual segregation in the scalloped hammerhead shark, *Sphyrna lewini*. *Environmental Biology of Fishes, 18,* 27–40.

Koenig, A. E. & Wilson, S. A. (2007). A marine carbonate reference material for microanalysis. In Proceedings of the First International Sclerochronology Conference, St. Petersburg, Florida, July 17–21, 2007.

Kotas, J. E., Mastrochirico, V. & Petrere Junior, M. (2011). Age and growth of the scalloped hammerhead shark, *Sphyrna lewini* (Griffith and Smith, 1834), from the southern Brazilian coast. *Brazilian Journal of Biology, 71,* 755–761.

Kotas, J. E., Petrere Junior, M., Dos Santos, R. A., Bustamante, A., Lin, C. F., Da Silveira Menezes, A. A. & Veras Micheletti, E. L. (2014). The horizontal migration of hammerhead sharks along the southern Brazilian coast, based on their exploitation pattern and considerations about the impact of anchored gillnets activities on these Species. *Revista CEPSUL - Biodiversidade e Conservação Marinha*, *3*, 45–68.

Lewis, J. P., Patterson, W. F., Carlson, J. K. & McLachlin, K. (2016). Do vertebral chemical signatures distinguish juvenile blacktip shark (*Carcharhinus limbatus*) nursery regions in the northern Gulf of Mexico*? Marine and Freshwater Research, 67,* 1014–1022.

Licandeo, R. & Cerna, F. T. (2007). Geographic variation in life-history traits of the endemic kite skate *Dipturus chilensis* (Batoidea: Rajidae), along its distribution in the fjords and channels of Southern Chile. *Journal of Fish Biology, 71,* 421–440.

Limbeck, A., Galler, P., Bonta, M., Bauer, G., Nischkauer, W. & Vanhaecke, F. (2015). Recent advances in quantitative LA-ICP-MS analysis: Challenges and solutions in the life sciences and environmental chemistry. *Analytical and Bioanalytical Chemistry, 407*, 6593–6617.

Lombardi-Carlson, L. A., Cortés, E., Parsons, G. R. & Manire, C. A. (2003). Latitudinal variation in life-history traits of bonnethead sharks, *Sphyrna tiburo*, (Carcharhiniformes:Sphyrnidae) from the Eastern Gulf of Mexico. *Marine and Freshwater Research, 54,* 875–883.

McMillan, M. N., Izzo, C., Wade, B. & Gillanders, B. M. (2017). Elements and elasmobranchs: hypotheses, assumptions and limitations of elemental analysis. *Journal of Fish Biology, 90,* 559–594.

McMillan, M. N., Huveneers, C., Semmens, J. M. & Gillanders, B. M. (2018). Natural tags reveal populations of conservation dependent school shark use different pupping areas. *Marine Ecology Progress Series, 599,* 147–156.

Mohan, J. A., Miller, N. R., Herzka, S. Z., Sosa-Nishizaki, O., Kohin, S., Dewar, H., Kinney, M., Snodgrass, O. & Wells, R. J. D. (2018). Elements of time and place: manganese and barium in shark vertebrae reflect age and upwelling histories. *Proceedings of the Royal Society B, 285*, 1–7.

Nakano, H. & Stevens, J. (2008). The Biology and Ecology of the Blue Shark, *Prionace glauca.* In Sharks of the Open Ocean: Biology, Fisheries and Conservation (M Camhi, E Pikitch, E. B., ed), pp. 140–151 Oxford, UK: Blackwell Publishing.

Natanson, L. J. & Cailliet, G. M. (1990). Vertebral growth zone deposition in pacific angel sharks. *Copeia, 4,* 133–1145.

Natanson, L. J. (1993). Effect of temperature on band deposition in the little skate, *Raja erinacea. Copeia, 1*, 199–206.

Natanson, L. J., Casey, J. G. & Kohler, N. E. (1995). Age and growth estimates for the dusky shark, *Carcharhinus obscurus*, in the western north Atlantic Ocean. *Oceanographic Literature Review, 9,* 786.

Natanson, L. J., Wintner, S. P., Johansson, F., Piercy, A., Campbell, P., De Maddalena, A., Gulak, S. J. B., Human, B., Fulgosi, F. C., Ebert, D. A., Hemida, F., Mollen, F. H., Vanni, S., Burgess, G. H., Compagno, L. J. V. & Wedderburn-Maxwell, A. (2008). Ontogenetic vertebral growth patterns in the basking shark *Cetorhinus maximus*. *Marine Ecology Progress Series, 361*, 267–278.

Okamura, H. & Semba, Y. (2009). A novel statistical method for validating the periodicity of vertebral growth band formation in elasmobranch fishes. *Canadian Journal of Fisheries and Aquatic Sciences, 66*, 771–780.

Okamura, H., Punt, A. E., Semba, Y. & Ichinokawa, M. (2013). Marginal increment analysis: a new statistical approach of testing for temporal periodicity in fish age verification. *Journal of Fish Biology, 82,* 1239–1249.

Parsons, G. R. (1993). Age determination and growth of the bonnethead shark *Sphyrna tiburo:* a comparison of two populations. *Marine Biology, 117,* 23–31.

Passerotti, M. S., Carlson, J. K., Piercy, A. N. & Campana, S. E. (2010). Age validation of great hammerhead shark (*Sphyrna mokarran*), determined by bomb radiocarbon analysis. *Fishery Bulletin, 108,* 346–351.

Pearce, N. J. G., Perkins, W. T., Westgate, J. A., Gorton, M. P., Jackson, S. E., Neal, C. R. & Chenery, S. P. (1997). A compilation of new and published major and trace element data for NIST SRM 610 and NIST SRM 612 glass reference materials. *Geostandards and Geoanalytical Research, 21,* 115–144.

Piercy, A. N., Carlson, J. K., Sulikowski, J. A. & Burgess, G. H. (2007). Age and growth of the scalloped hammerhead shark, *Sphyrna lewini*, in the north-west Atlantic Ocean and Gulf of Mexico. *Marine and Freshwater Research, 58*, 34–40.

Pistevos, J. C. A., Nagelkerken, I., Rossi, T., Olmos, M. & Connell, S. D. (2015). Ocean acidification and global warming impair shark hunting behaviour and growth. *Scientific Reports, 5,* 16293.

Pratt, H. & Casey, G. (1983). Age and growth of the shortfin mako, *Isurus oxyrinchus*, using four methods. *Canadian Journal of Fisheries and Aquatic Sciences, 40,* 1944–1957.

Raoult, V., Peddemors, V. M., Zahra, D., Howell, N., Howard, D. L., de Jonge, M. D. & Williamson, J. E. (2016). Strontium mineralisation of shark vertebrae. *Scientific Reports, 6,* 29698.

Ribot-Carballal, M. C., Galván-Magaña, F. & Quiñónez-Velázquez, C. (2005). Age and growth of the shortfin mako shark, *Isurus oxyrinchus*, from the western coast of Baja California Sur, Mexico. *Fisheries Research, 76,* 14–21.

Scharer, R. M., Patterson, W. F., Carlson, J. K. & Poulakis, G. R. (2012). Age and growth of endangered smalltooth sawfish (*Pristis pectinata*) verified with LA-ICP-MS analysis of vertebrae. *PLoS ONE, 7,* 1–8.

Schroeder, R. (2011) Utilisation of vertebral microchemistry techniques to determine population structure of two inshore shark species along the east coast of Queensland, Australia. Master thesis, James Cook University.

Sepulveda, C. A., Kohin, S., Chan, C., Vetter, R. & Graham, J. B. (2004). Movement patterns, depth preferences and stomach temperatures of free-swimming juvenile mako sharks, *Isurus oxyrinchus*, in the Southern California bight. *Marine Biology, 145*, 191–199.

Sinclair, D. J., Kinsley, L. P. J. & Mcculloch, M. T. (1998). High resolution analysis of trace elements in corals by laser ablation ICP-MS. *Geochimica et Cosmochimica Acta, 62,* 1889–1901.

Smith, W. D., Miller, J. A. & Heppell, S. S. (2013). Elemental markers in elasmobranchs: effects of environmental history and growth on vertebral chemistry. *PLoS ONE, 8,* e62423.

Smith, W. D., Miller, J. A., Márquez-Farías, J. F. & Heppell, S. S. (2016). Elemental signatures reveal the geographic origins of a highly migratory shark: prospects for measuring population connectivity. *Marine Ecology Progress Series, 556,* 173–193.

Tillett, B. J., Meekan, M. G., Parry, D., Munksgaard, N., Field, I. C., Thorburn, D. & Bradshaw, C. J. (2011). Decoding fingerprints: elemental composition of vertebrae correlates to age-related habitat use in two morphologically similar sharks. *Marine Ecology Progress Series, 434,* 133–142.

Torres-Huerta, A. M., Villavicencio-Garayzar, C. & Corro-Espinosa, D. (2008). Reproductive biology of the scalloped hammerhead shark *Sphyrna lewini* Griffith & Smith (Sphyrnidae) in the Gulf of California. *Hidrobiologica, 18,* 227–237.

Urist, M. R. (1961). Calcium and phosphorus in the blood and skeleton of the Elasmobranchii. *Endocrinology, 69,* 778–801.

Wells, R. J. D., Smith, S. E., Kohin, S., Freund, E., Spear, N. & Ramon, D. A. (2013). Age validation of juvenile shortfin mako (*Isurus oxyrinchus*) tagged and marked with oxytetracycline off Southern California. *Fishery Bulletin, 111,* 147–160.

Wells, R. J. D., Spear, N. & Kohin, S. (2017). Age validation of the blue shark (*Prionace glauca*) in the Eastern Pacific Ocean. *Marine and Freshwater Research, 68,* 1130–1136.

**TABLE 1** Number of peaks counted in the smoothed profiles of the $^{43}$Ca raw counts $s^{-1}$ data and $^{31}$P:Ca and $^{55}$Mn:Ca, obtained from LA-ICP-MS transect scans encompassing the area from the focus to the edge of the vertebrae from 15 juvenile *Sphyrna lewini*, compared with the number of opaque growth bands.

| Sampling site | Sampling date | Sample | Total length (cm) | Sex | Opaque growth bands (*n*) | $^{43}$Ca peak (*n*) | $^{31}$P:Ca peak (*n*) | $^{55}$Mn:Ca peak (*n*) |
|---|---|---|---|---|---|---|---|---|
| La Reforma | April 2015 | RE-1 | 84 | ♂ | 3 | 2 | 5 | 5 |
| | | RE-2 | 86.8 | ♂ | 3 | 2 | 7 | 1 |
| | | RE-3 | 90.8 | ♂ | 3* | 3* | 4 | 5 |
| | | RE-4 | 84.4 | ♀ | 3* | 4 | 4 | 3* |
| | | RE-5 | 71.2 | ♂ | 2* | 2* | 2* | 2* |
| Chametla | November 2014 | CH-1 | 72.8 | ♂ | 2* | 1 | 1 | 2* |
| | | CH-2 | 83 | ♀ | 2* | 2* | 3 | 2* |
| | | CH-3 | 87 | ♂ | 4 | 5 | 6 | 3 |
| | | CH-4 | 83 | ♀ | 2* | 3 | 3 | 2* |
| | | CH-5 | 83 | ♂ | 5* | 0 | 5* | 5* |
| Teacapán | Febeuary 2014 | TC-1 | 78.2 | ♂ | 4* | 3 | 4* | 4* |
| | | TC-2 | 84 | ♂ | 4* | 4* | 4* | 3 |
| | | TC-3 | 69 | ♀ | 2* | 1 | 2* | 2* |
| | | TC-4* | 66.4 | ♀ | 2* | 1 | 2* | 2* |
| | | TC-5 | 66.6 | ♀ | 1* | 1* | 1* | 1* |

*Samples with peak counts that corresponded with the number of opaque growth bands. (See Figure 7 for the illustration of the corresponding elemental profiles.)

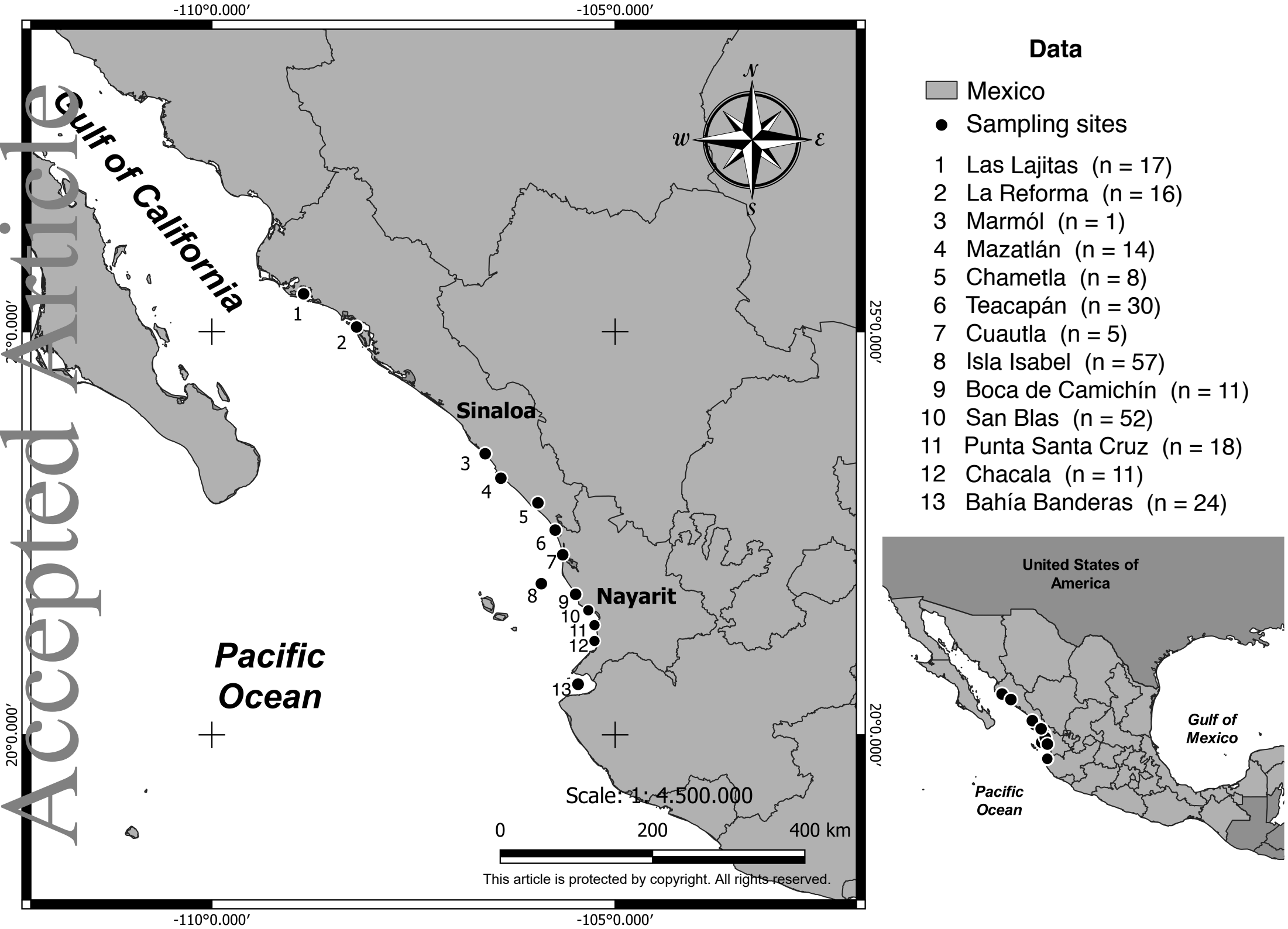

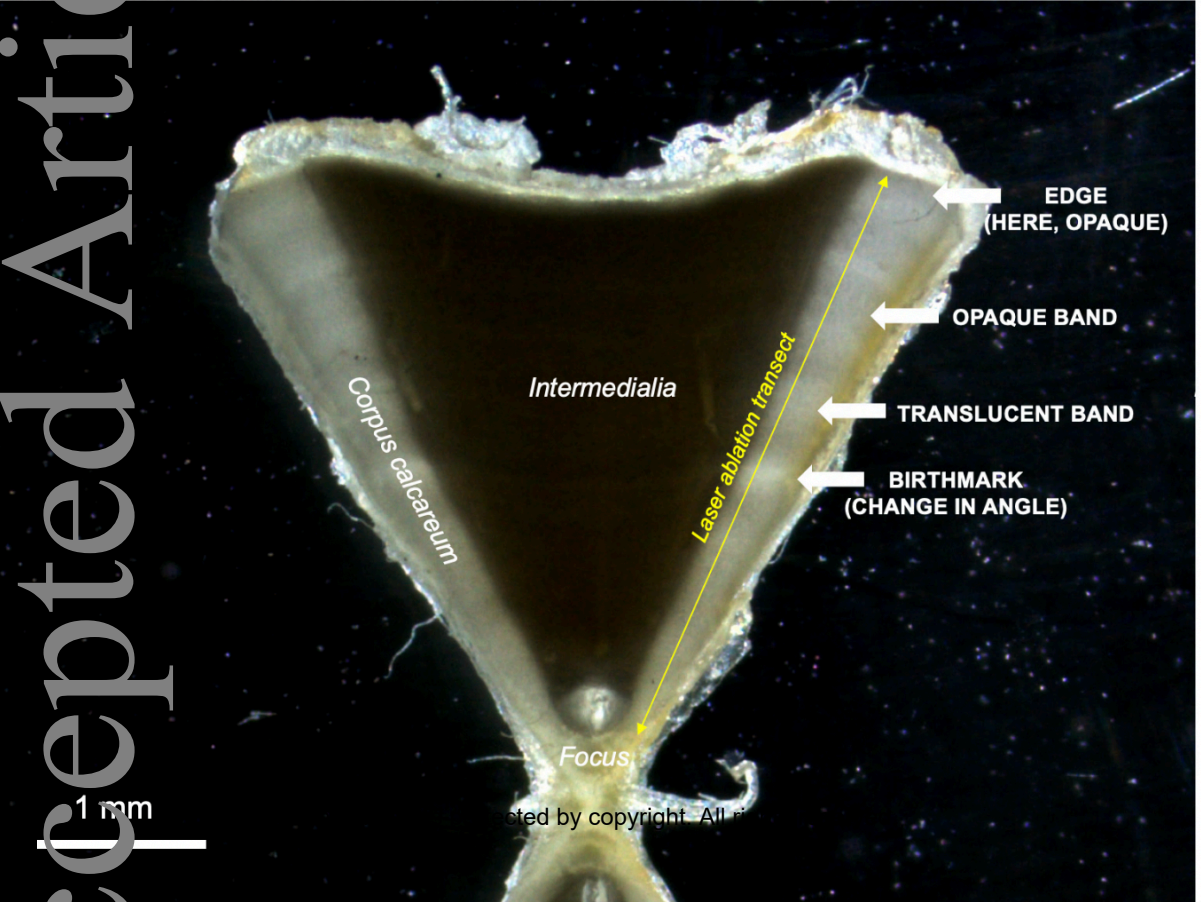

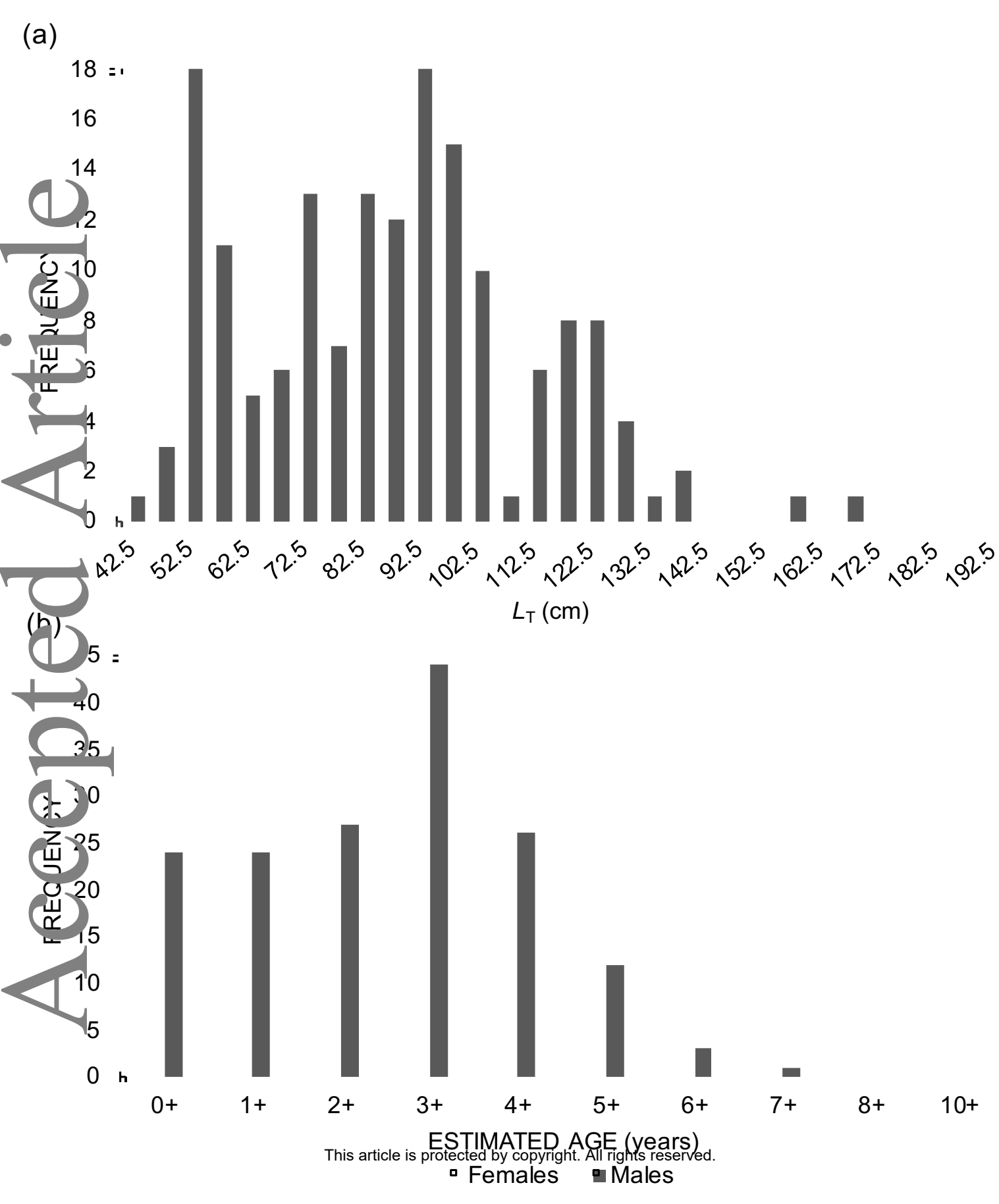

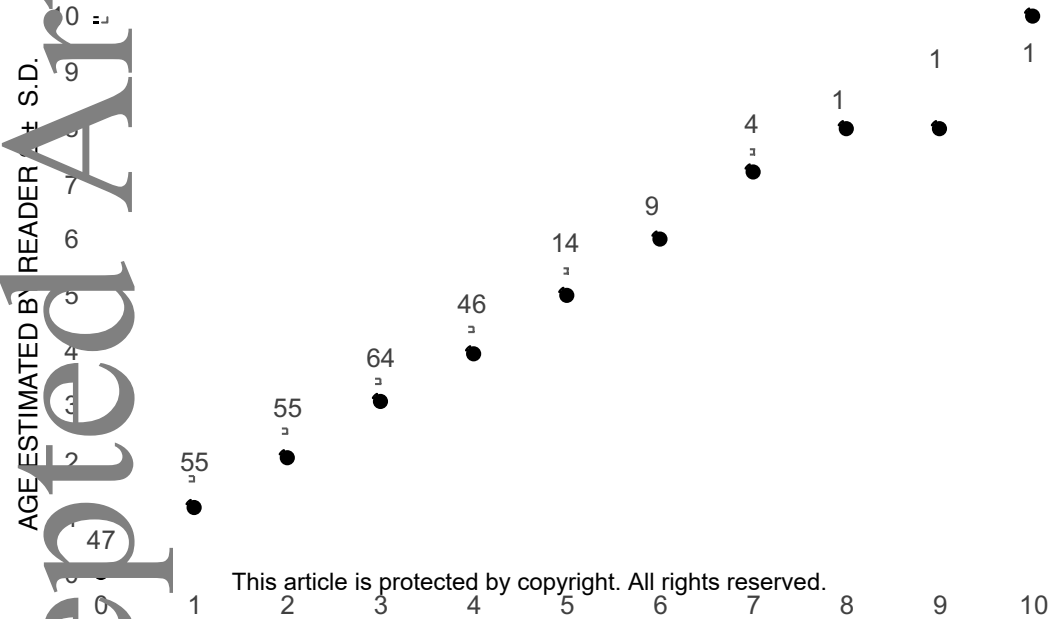

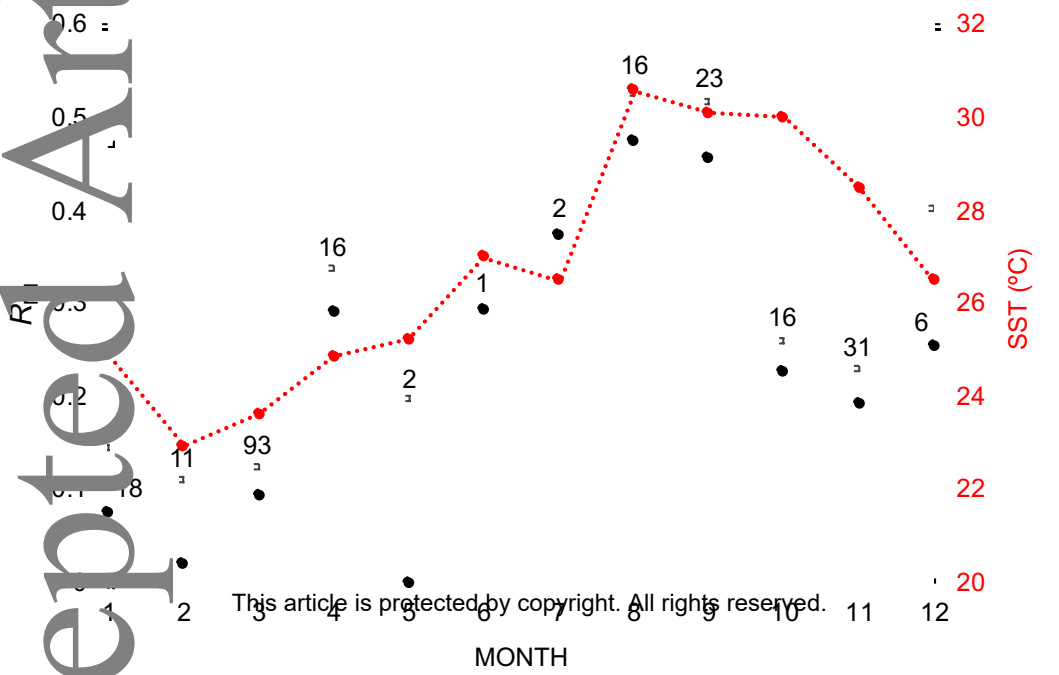

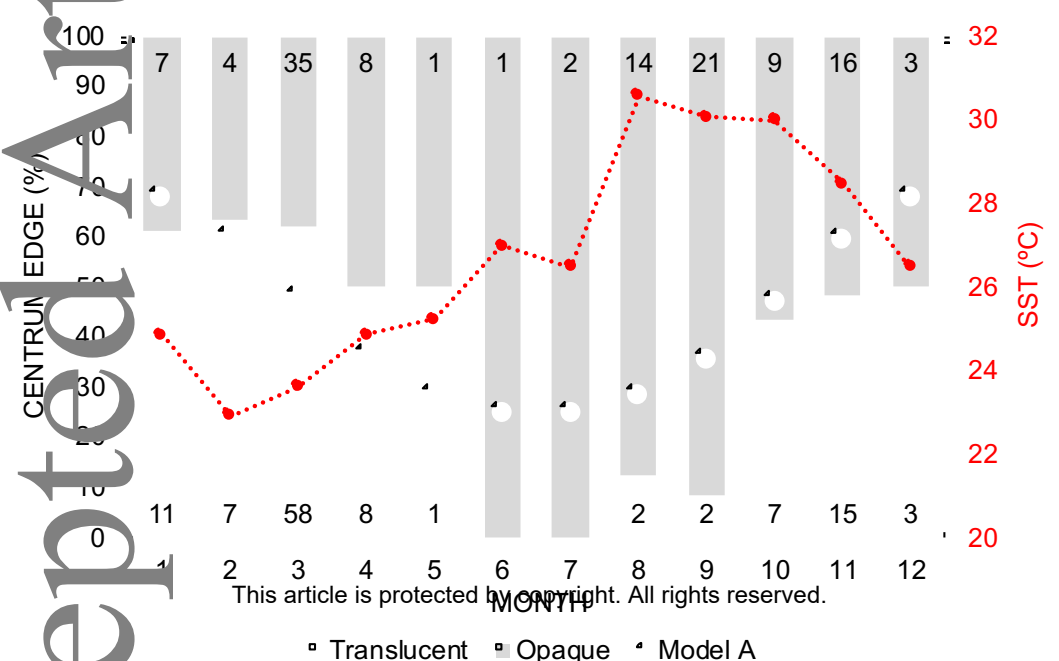

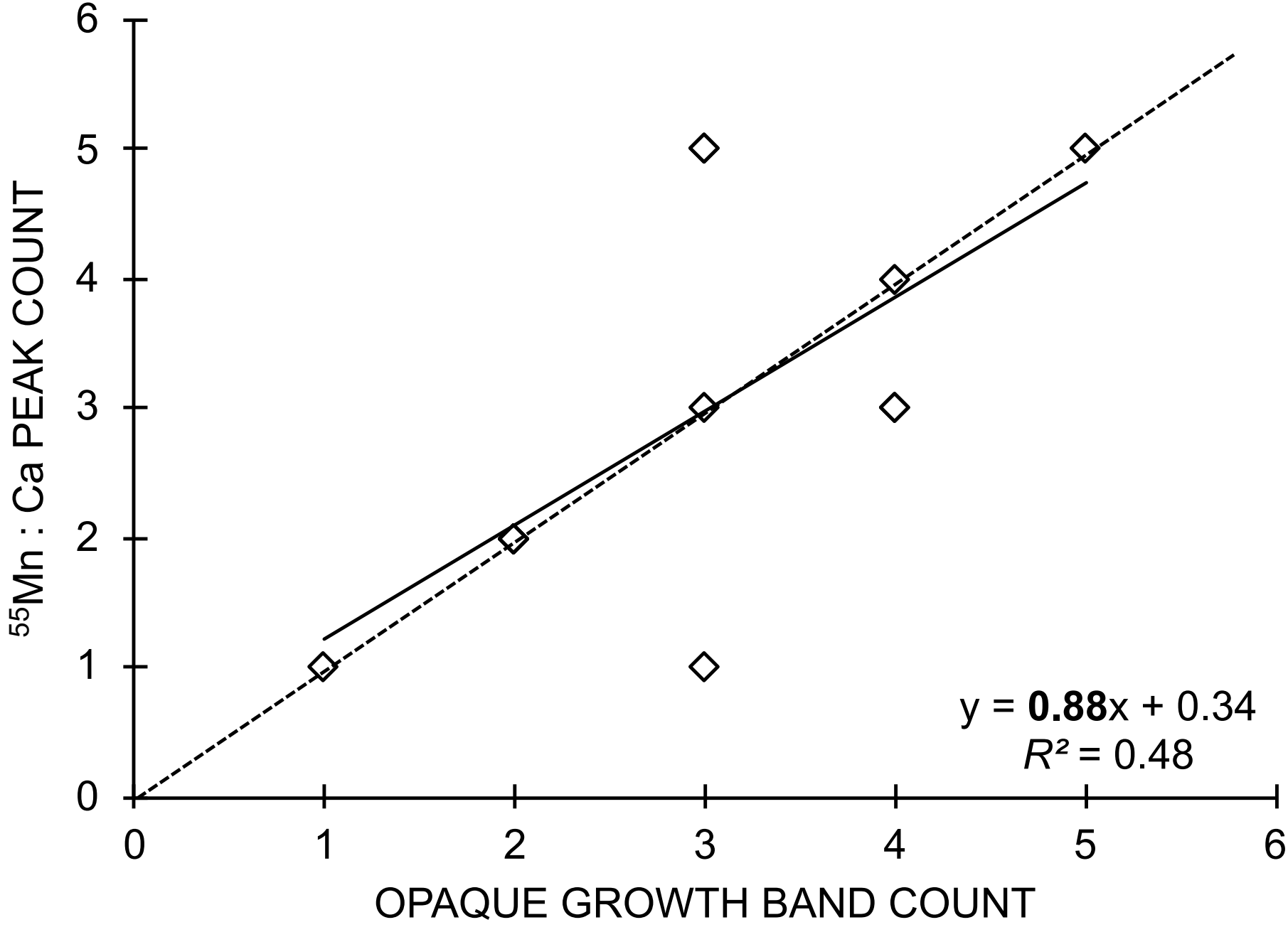
6
5
4
3
2
1
0
$^{55}$Mn : Ca PEAK COUNT
0
1
2
3
4
5
6
OPAQUE GROWTH BAND COUNT
y = **0.88**x + 0.34
$R^2$ = 0.48

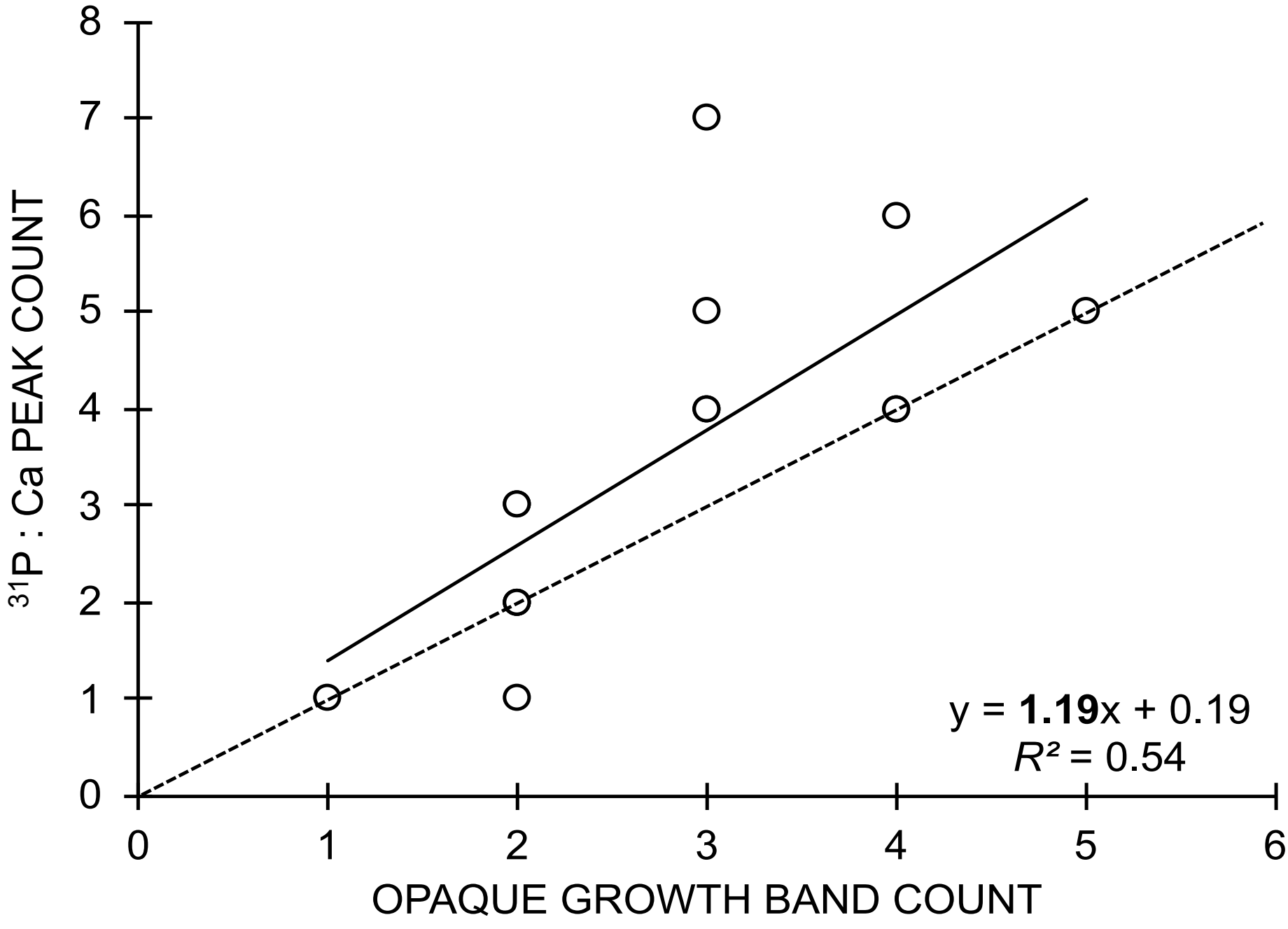
8
7
6
5
4
3
2
1
0
$^{31}$P : Ca PEAK COUNT
0
1
2
3
4
5
6
OPAQUE GROWTH BAND COUNT
y = **1.19**x + 0.19
$R^2$ = 0.54

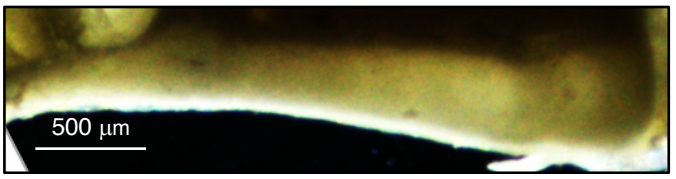


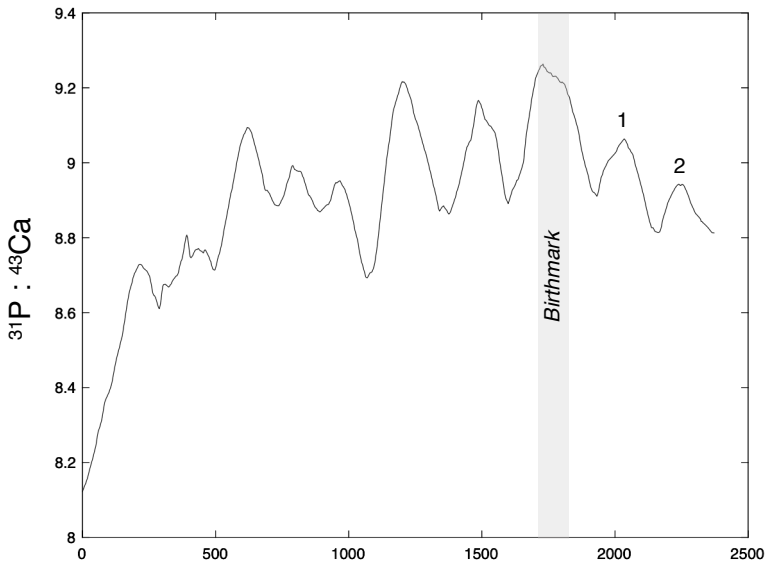


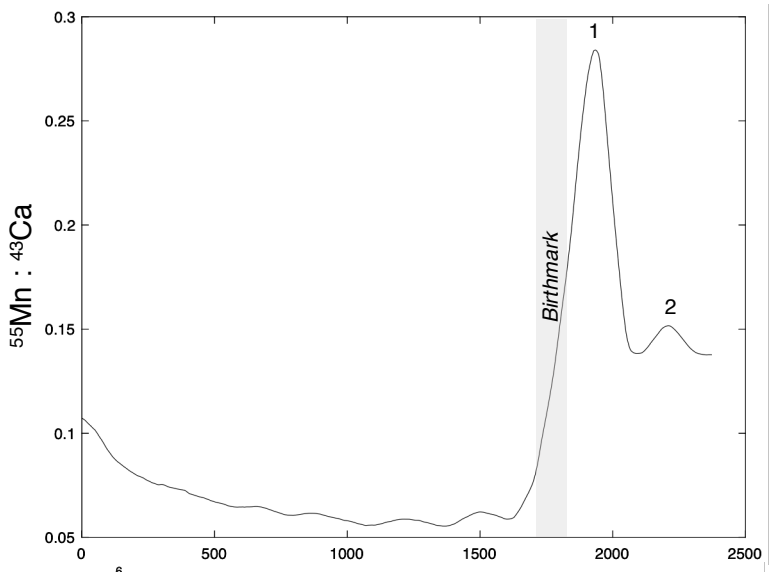


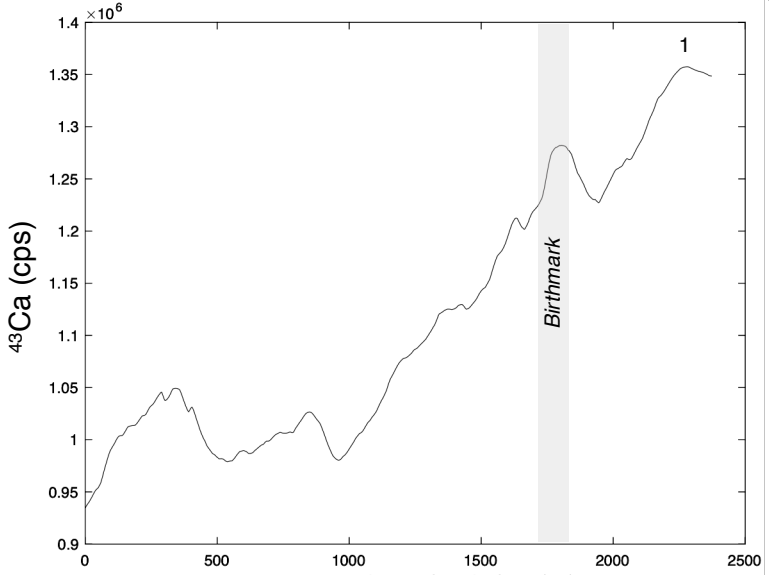


Laser transect distance from the focus (µm)